Seismic performance of zero-gap pounding tuned mass dampers

30th International Congress on Sound and Vibration

ICSV30 AMSTERDAM 8-11 JULY 2024

SEISMIC PERFORMANCE OF ZERO-GAP POUNDING TUNED MASS DAMPERS

Emiliano Matta
Politecnico di Torino, Torino, Italy
email: emiliano.matta@polito.it

As a recent variant of the classical viscous tuned mass damper (VTMD), the pounding tuned mass damper (PTMD) relies on impact with the main structure as the source of energy dissipation. Unlike the symmetrical double-sided PTMD, the asymmetrical single-sided PTMD appears especially promising because of its limited sensitivity to the excitation amplitude. However, a thorough assessment of its performance is still lacking, particularly under seismic loading. In this paper, a single-sided PTMD having zero impact gap in the undeformed state is investigated under the assumption of a stereo-mechanical non-smooth impact model. First, its mathematical model is derived and proved to be nonlinear but homogeneous, which ensures an amplitude-independent effectiveness on linear structures. In this light, an H_∞- and an H_2-optimum design strategies are then proposed for a PTMD on a single-degree-of-freedom linear structure, whereby the optimal PTMD is determined by minimizing, respectively, the H_∞ and the H_2 norm of the input-output transfer function from the ground acceleration to the structural displacement, approximated by numerical simulations under repeated sinusoidal and white noise excitations. The obtained H_∞- and H_2-optimum PTMDs are finally compared with the corresponding H_∞- and H_2-optimum VTMDs, considering various mass ratios and several input types (including a large set of natural seismic records), and admitting possible undesired changes of the structural frequency. The results show that the PTMD is generally less effective than the VTMD if the structure responds as nominally expected, but sensibly more effective in the event of structural variations. They also show that the H_∞ design is less effective than the H_2 design in nominal conditions, but more robust against uncertainties. In conclusion, the zero-gap PTMD proves a promising alternative to traditional TMD types, and this study offers simple and effective solutions for its optimal seismic design.

Keywords: seismic control, TMD, pounding, amplitude independence, homogeneous nonlinearity

1. Introduction

Tuned mass dampers (TMDs) are well-known passive vibration control devices. The classical TMD is a single-degree-of-freedom (SDOF) linear oscillator appended to the main structure and tuned to one target structural mode. If optimally tuned to the target mode by an appropriate setting of its frequency and damping ratio, the TMD adsorbs and dissipates part of the vibrational energy in that mode, thus reducing the structural response. If the TMD mass ratio is large enough, significant reductions are achievable also in the face of non-stationary loads such as earthquake ground motions [1]. However, severe losses of control performance may be caused by detuning, possibly occurring during seismic events as a consequence of damage-induced reductions in the structural frequencies [2].

The classical linear TMD relies on linear viscous dampers as a source of energy dissipation, and is therefore herein denoted as the viscous TMD (VTMD). The potential drawbacks inherent in viscous

dampers (sensitivity to temperature, response nonlinearity, encumbrance, construction and maintenance cost) justify the search for alternative dissipative sources, including friction, metallic yielding and visco-elastic damping [3]. Among these, impact dissipation is exploited in the pounding TMD (PTMD) [4]. In a PTMD, impact occurs between the TMD mass and the main structure, with or without interposition of a viscoelastic layer, whenever the TMD stroke exceeds the available gap. Earliest examples of PTMDs present a symmetrical arrangement with a double-sided (DS) gap, featuring two impacts per cycle of TMD oscillation. Effective for a given excitation amplitude, DS-PTMDs prove under-damped for lower amplitudes and over-damped for larger ones. Later variants present an asymmetrical arrangement with a single-sided (SS) gap, featuring one impact per cycle [5]. Compared with DS-PTMDs, SS-PTMDs require larger dissipation per impact but their performance is less dependent on the excitation level. Among SS-PTMDs, particularly interesting is the zero-gap PTMD [6]. With the gap being annulled in the at-rest position, a zero-gap PTMD is simpler to design and scarcely affected by the excitation level. However, a full understanding of its potential is still lacking, particularly in seismic applications.

In this paper, the zero-gap PTMD is studied for application on a SDOF linear structure under ground motion, and its performance is compared with that of an ordinary VTMD. At first, the PTMD mathematical model is derived assuming a stereo-mechanical impact model, and is proven to be nonlinear but homogeneous, which makes the effectiveness of the PTMD unaffected by the input amplitude. Secondly, for both the VTMD and the PTMD, the optimal design problem is set in the framework of the classical H_∞ and H_2 norm design methods. Thirdly, the H_∞ and H_2 optimum solutions are determined for both TMD types and for a large range of possible mass ratios. Finally, also admitting possible changes in the value of the structural frequency, the effectiveness and robustness of the two types are compared under the effect of several base acceleration time-histories, including sinusoidal actions, white noise actions and a large set of natural seismic records. Conclusions are drawn at last, highlighting the pros and cons of the PTMD device with respect to the traditional VTMD solution.

2. The mathematical model

The model of a TMD on a SDOF linear structure is schematized in Fig. 1, supposing that its dissipation incorporates both linear viscous and nonlinear impact damping. In it, m_s, k_s and c_s are, respectively, the mass, stiffness and damping coefficient of the main structure; m, k and c are the mass, stiffness and damping coefficient of the TMD; e is the restitution coefficient at the structure-TMD interface; $u_g(t)$ is the ground horizontal absolute displacement; $u_s(t)$ is the structure horizontal displacement relative to the ground; $u(t)$ is the TMD horizontal displacement relative to the structure; and u_c is the clearance of the TMD-structure gap, measured when the TMD is in its at-rest position (i.e. when $u(t) = 0$).

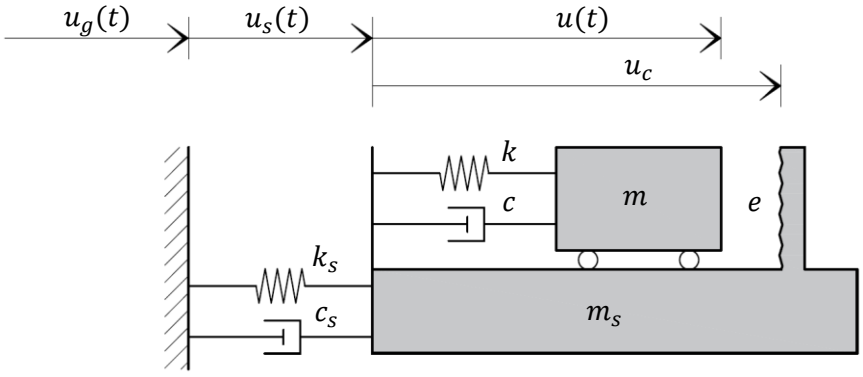

Figure 1: The mathematical model.

The dynamic equations for such a system are as follows:

$$\begin{cases} m_s(\ddot{u}_g + \ddot{u}_s) + c_s\dot{u}_s + k_s u_s = ku + f_d \\ m(\ddot{u}_g + \ddot{u}_s + \ddot{u}) + ku + f_d = 0 \end{cases} \tag{1}$$

where

$$f_d = f_c + f_p \tag{2}$$

is the dissipative force exerted by the TMD onto the structure, including the viscous damping force f_c transmitted through the linear viscous damper and the pounding force f_p transmitted through the impact interface. While the viscous force is $f_c = c\dot{u}$, the pounding force is here defined using a classical non-smooth, stereo-mechanical impact model, whereby the impact is instantaneous and governed by the restitution coefficient e, ranging from 0 (perfectly plastic impact) to 1 (perfectly elastic impact).

Considering Fig. 1, a non-smooth impact occurs at the time instant t_c if at that instant:

$$u = u_c \quad \text{and} \quad \dot{u}^- > 0 \tag{3}$$

where the superscript "–" denotes the pre-impact state of the system, as the superscript "+" will denote in the sequel the post-impact state.

If Eqs. (3) hold and the TMD mass ratio is introduced as $m_R = m/m_s$, then the relative velocities of, respectively, the TMD and the structure will change at the instant t_c according to:

$$\dot{u}^+ = -e\dot{u}^- \tag{4}$$

$$\dot{u}_s{}^+ = \dot{u}_s{}^- + \frac{1+e}{1+\frac{1}{m_R}}\dot{u}^- \tag{5}$$

At the instant t_c an impulse is then transmitted by the TMD to the structure equal to:

$$J = m_s(\dot{u}_s{}^+ - \dot{u}_s{}^-) = m\frac{1+e}{1+m_R}\dot{u}^- \tag{6}$$

which makes the corresponding pounding force f_p impulsive and representable as:

$$f_p^i = m\frac{1+e}{1+m_R}\dot{u}^-\delta(t - t_c) \geq 0 \tag{7}$$

where $\delta(t - t_c)$ is the Dirac delta function, and the superscript "i" stands for "impulsive".

If, instead, during a certain time interval, the TMD is stuck to the structure according to:

$$u = u_c \quad \text{and} \quad \dot{u}^- = 0 \tag{8}$$

a smooth compressive contact force will be transmitted by the TMD to the structure during that interval so as to prevent the condition $\ddot{u} > 0$ (implying interpenetration of TMD and structure), expressed by:

$$f_p^s = \max[\,0\,;\, \frac{m_R(c_s\dot{u}_s + k_s u_s)}{(1+m_R)} - ku\,] \geq 0 \tag{9}$$

where the superscript "s" stands for "smooth".

By combining Eqs. (7) and (9), the force at the pounding interface is finally obtained as:

$$f_p = \begin{cases} f_p^i \;, & if\ u = u_c \text{ and } \dot{u}^- > 0 \\ f_p^s \;, & if\ u = u_c \text{ and } \dot{u}^- = 0 \end{cases} \tag{10}$$

The above model is valid for a TMD with both viscous and pounding dissipation, but will be used in the sequel to separately represent either a VTMD (by annulling f_p) or a PTMD (by annulling f_c). Additionally, the above pounding model is valid for any value of u_c, but will be used in the sequel only to represent zero-gap PTMDs, having $u_c = 0$.

Fundamentally, if and only if $u_c = 0$, the force f_p in Eqs. (10) is a homogeneous function of the state vector $\boldsymbol{x} = \{ u_s ,\ u ,\ \dot{u}_s ,\ \dot{u} \}'$, in that $f_p(\gamma \boldsymbol{x}) = \gamma f_p(\boldsymbol{x})\ \forall\ \gamma \in R$. For the zero-gap PTMD, therefore, Eqs. (1) are nonlinear but homogeneous equations, and the response of the structure-PTMD system is proportional to the amplitude of the excitation. Such response can be numerically obtained by recasting Eqs. (1) into a system of first-order nonlinear differential equations in the state variables, and by integrating them using a Runge-Kutta algorithm.

3. The optimal design methodology

Optimization is here set according to two possible design criteria: (i) the H_∞ design, minimizing the worst-case steady-state structural response to a unit-amplitude harmonic input; and (ii) the H_2 design, minimizing the root-mean-square (rms) structural response to a stationary Gaussian zero-mean white-noise input. To do so, it is first convenient to reshape Eqs. (1) in modal terms as follows:

$$\begin{cases} \ddot{u}_s + 2\zeta_s\omega_s\dot{u}_s + \omega_s^2 u_s = m_R\left(\omega_R^2\omega_s^2 u + 2\zeta\omega_R\omega_s\dot{u} + \frac{f_p}{m}\right) - \ddot{u}_g \\ \ddot{u} + \omega_R^2\omega_s^2 u + 2\zeta\omega_R\omega_s\dot{u} + \frac{f_p}{m} = -\ddot{u}_s - \ddot{u}_g \end{cases} \tag{11}$$

where

$$\frac{f_p}{m} = \begin{cases} \frac{1+e}{1+m_R}\dot{u}^-\delta(t-t_c) \quad , \quad if\ u = 0 \text{ and } \dot{u}^- > 0 \\ \max[\ 0\ ;\ \frac{2\zeta_s\omega_s\dot{u}_s + \omega_s^2 u_s}{1+m_R} - \omega_R^2\omega_s^2 u\ ]\ , \quad if\ u = 0 \text{ and } \dot{u}^- = 0 \end{cases} \tag{12}$$

In Eqs. (11) and (12), $\omega_s = \sqrt{k_s/m_s}$ and $\zeta_s = c_s/(2\omega_s m_s)$ are the circular frequency and the damping ratio of the main structure; $\omega_R = \omega/\omega_s$ is the frequency ratio, with $\omega = \sqrt{k/m}$ being the circular frequency of the TMD; and $\zeta = c/(2\omega m)$ is the viscous damping ratio of the TMD.

According to Eqs. (11) and (12), once the structure and the external input are assigned, the response of the system entirely depends on the four dimensionless parameters m_R, ω_R, ζ and e. Assuming the structure known and m_R established, the only two available free parameters, i.e. ω_R and ζ for the VTMD and ω_R and e for the PTMD, are determined by minimizing either the H_∞ or the H_2 norm of a selected input-output transfer function (TF). Choosing the ground acceleration $\ddot{u}_g$ as the input and the structural relative displacement u_s as the output, $T_{u_s\ddot{u}_g}(\omega_g)$ is the adopted TF, where ω_g is the circular frequency of the input. Introducing the response ratio $R = \left\|T_{u_s\ddot{u}_g}\right\|_n^{con} \Big/ \left\|T_{u_s\ddot{u}_g}\right\|_n^{unc}$ as the ratio of the controlled to the uncontrolled H_n norm of $T_{u_s\ddot{u}_g}(\omega_g)$ (n standing either for ∞ or for 2), the H_∞ and the H_2 optimization problems can each be formalized as follows:

$$R_{opt} = \min_{\omega_R,\zeta} R\ , \quad \text{for the VTMD} \tag{13}$$

$$R_{opt} = \min_{\omega_R,e} R\ , \quad \text{for the PTMD} \tag{14}$$

which respectively provide the VTMD optimal parameters, ω_{Ropt} and ζ_{opt}, and the PTMD optimal parameters, ω_{Ropt} and e_{opt}. Because R only depends on the structural damping ratio ζ_s and on the dimensionless TMD parameters, the solutions to Eqs. (13) and (14) exclusively depend on ζ_s and m_R.

While the solution to Eq. (13) is already known, Eq. (14) is new, and here numerically solved using a branch and bound algorithm. To this aim, the objective function R must be computed in an approximate way for the nonlinear system in Eq. (14). In the H_∞ case, the TF is computed by points, through simulating the system separately under each harmonic input frequency, until stabilization of the response amplitude.

In the H_2 case, the stationary rms response is computed through Monte Carlo simulations, i.e. by averaging the rms response of the system to many realizations of the stochastic input process.

For $\zeta_s = 2\%$ and $m_R = 10\%$, the H_∞-optimal VTMD and PTMD are compared in Fig. 2. In Fig. 2a, both TFs have the typical two-peak shape due to TMD-structure coupling, but the TF for the PTMD is higher and exhibits additional peaks due to the PTMD sub-harmonics. In Figs. 2b to 2d, the time response is shown under the first 15 cycles of a sinusoidal input $\ddot{u}_g = \ddot{u}_{g0}\sin(\omega_s t)$ applied at the frequency of the main structure. For generality, displacements are normalized to the static displacement amplitude $u_{s0} = \ddot{u}_{g0}/\omega_s^2$, forces to the equivalent force amplitude $m_s\ddot{u}_{g0}$, and impulses to the equivalent momentum amplitude $m_s\,\ddot{u}_{g0}/\omega_s$. The steady-state time response, symmetric and smooth for the VTMD, is asymmetric and non-smooth for the PTMD, characterized by a unilateral (compressive) impulsive dissipative force, by a unilateral (negative) TMD relative displacement and by a slightly asymmetrical structural displacement. The H_∞ response appears larger for the PTMD (0.185) than for the VTMD (0.171), but not so much if compared with the uncontrolled response (1.000). Above all, it is amplitude-independent in all cases.

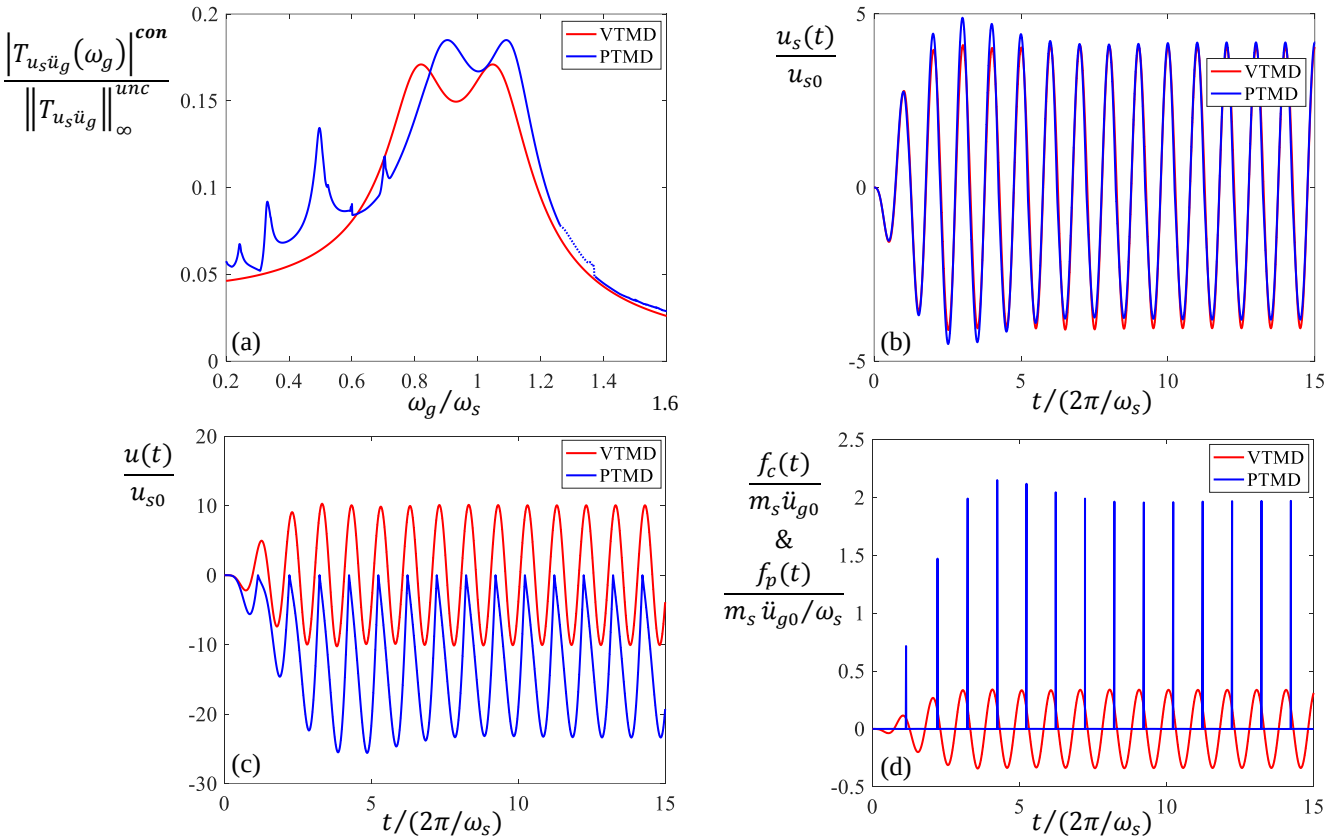

Figure 2: Frequency and time response of a structure-TMD system under harmonic input, for H_∞-optimal VTMD and PTMD having m_R = 10%: (a) TF; (b) structural displacement; (c) TMD displacement; (d) TMD dissipation.

By extending the H_∞ optimization to m_R ranging from 1‰ to 20%, and by repeating the procedure in H_2 terms, Fig. 3 is finally obtained, which provides the H_∞ and the H_2 optimal parameters and the corresponding response ratios, for both TMD types. Interestingly, for the PTMD it results that: (i) ω_{Ropt} is about 0.5 rather than about 1, as a result of the PTMD periodic motion occurring as a half-sine wave between impacts, rather than as a full-sine wave as for the VTMD; (ii) e_{opt} decreases approximately from 0.9 to 0.2 as m_R increases, as the a result of the TMD optimal damping increasing with m_R; and (iii) R_{opt} decreases with m_R as for the VTMD, but always remaining slightly larger.

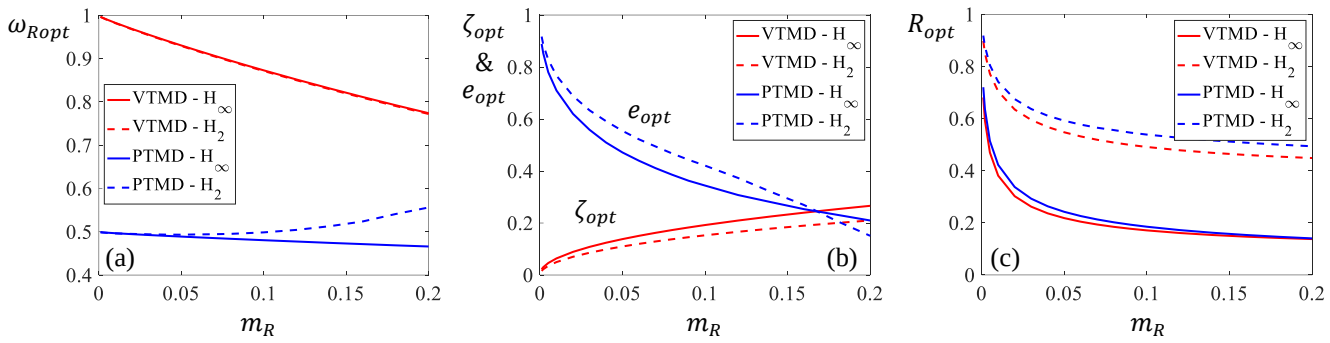

Figure 3: H_∞ and H_2 optimal design of VTMD and PTMD under ground acceleration as a function of m_R: (a) optimal frequency ratios; (b) optimal damping ratios and restitution coefficients; (c) optimal response ratios.

4. The seismic performance

With the VTMD and PTMD optimized alternatively in H_∞ and in H_2 terms (Figs. 3a and 3b), Eqs. (11) and (12) are now solved taking $\ddot{u}_g$ as a real seismic record. Simulations are repeated by imparting the structure an entire set of records, and by varying, for each record, the structural period T_s in the range 0.1÷6.0 s, so as to draw response spectra. The set is the one already used in [7], which includes 338 horizontal components of near-field records from the PEER NGA Strong Motion Database. Correspondingly, 338 spectra are obtained for each system configuration and for three response quantities herein chosen to depict the control performance, namely: (i) the maximum structural displacement $u_{s,max}$; (ii) the maximum required TMD stroke $\alpha \cdot u_{max}$, where $\alpha = 2$ for the VTMD and $\alpha = 1$ for the PTMD; (iii) the rms structural velocity $\dot{u}_{s,rms}$. For each configuration and for each response, the 338 spectra are first condensed into their respective rms spectrum, and then the following rms response ratio spectra are derived by dividing the controlled by the uncontrolled rms response spectra:

- $R_d = \text{rms}(u_{s,max})_{con} / \text{rms}(u_{s,max})_{unc}$
- $R_s = \text{rms}(\alpha \cdot u_{max})_{con} / \text{rms}(u_{s,max})_{unc}$
- $R_v = \text{rms}(\dot{u}_{s,rms})_{con} / \text{rms}(\dot{u}_{s,rms})_{unc}$

Results are shown in Fig. 4 assuming the H_2 design method and $m_R = 10\%$.

To further summarize the results, for each response ratio spectrum $R_{d/s/v}$ the mean spectral ratio $\bar{R}_{d/s/v}$ is obtained by averaging the spectral ordinates over the entire range of periods. Results are shown in Fig. 5 as a function of m_R, for the three responses, the two TMD types and the two design methods.

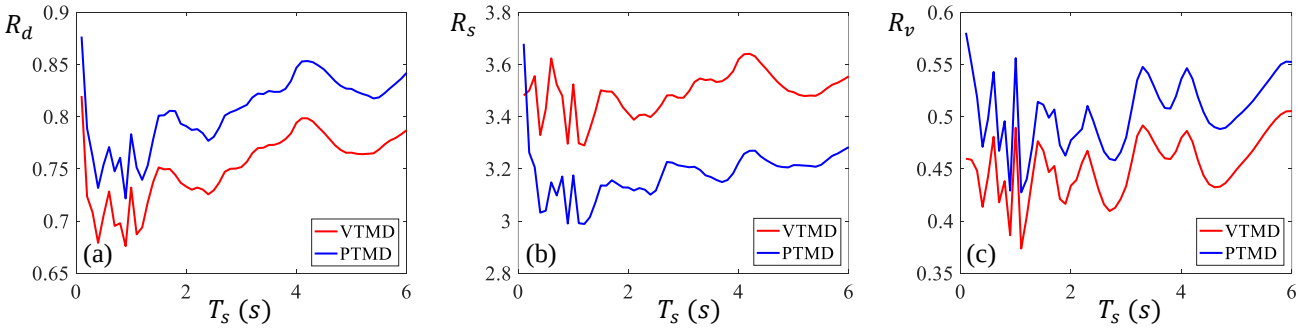

Figure 4: H_2-optimal VTMD and PTMD under the set of seismic records: rms response ratio spectra for $m_R = 10\%$, in terms of: (a) max structural displacement, (b) max TMD stroke, and (c) rms structural velocity.

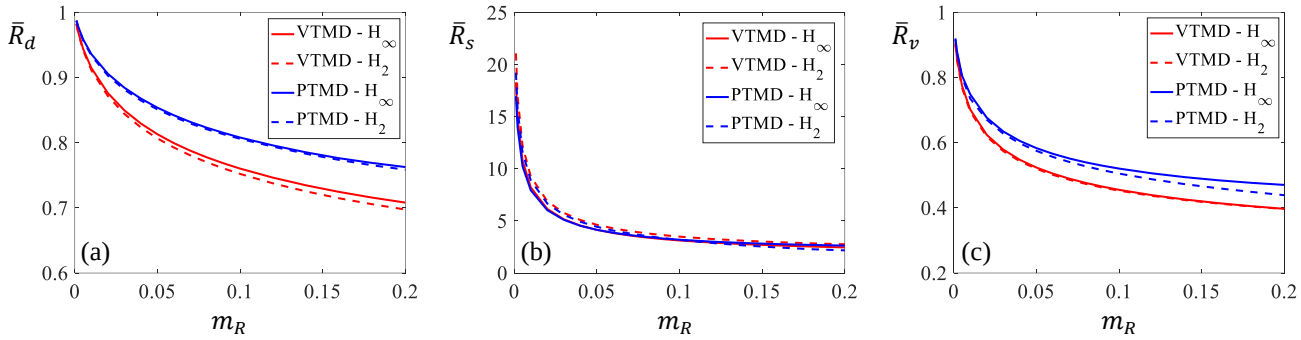

Figure 5: H_∞- and H_2-optimal VTMD and PTMD under the set of seismic records: mean spectral ratios as a function of m_R, in terms of: (a) max structural displacement, (b) max TMD stroke, and (c) rms structural velocity.

As for harmonic and white-noise excitation, the PTMD appears seismically less efficient than the VTMD, and the more so in reducing the peak response ($\bar{R}_d$) than in reducing the rms response ($\bar{R}_v$). Less remarkable is the difference in terms of TMD stroke ($\bar{R}_s$), slightly larger for the VTMD because of its larger effectiveness. Interestingly, the H_2 design outperforms the H_∞ design in all cases.

5. The robustness against detuning

One major drawback of TMDs is the degradation of their performance in the event of detuning, for instance induced by variations in the structural frequency or in the TMD damping ratio. In this paper, the robustness of VTMDs and PTMDs is investigated versus reductions in the natural frequency of the target mode, which may occur during and after seismic events. Namely, the "actual" structural circular frequency is assumed as $\omega_s = \omega_{s0}/\delta$, where ω_{s0} is the "nominal" structural circular frequency and δ is the frequency reduction factor. Values of δ equal to 1.2, 1.5 and 2.0 are adopted to represent small, medium and large variations, and the structure-TMD system is simulated assuming the structure as affected by such variations and the TMD as nominally designed.

Considering either a sinusoidal or a white-noise acceleration input, Fig. 6 shows how the optimal response ratio R_{opt} degrades as a consequence of δ with respect to the nominal case reported in Fig. 3c. Noticeably, the PTMD loses performance less rapidly than the VTMD. Regardless of the type of input, the PTMD shows a performance comparable with the nominal one, with R_{opt} always smaller than 1, whilst the VTMD shows a largely degraded performance, with R_{opt} even larger than 1 for $\delta = 2$.

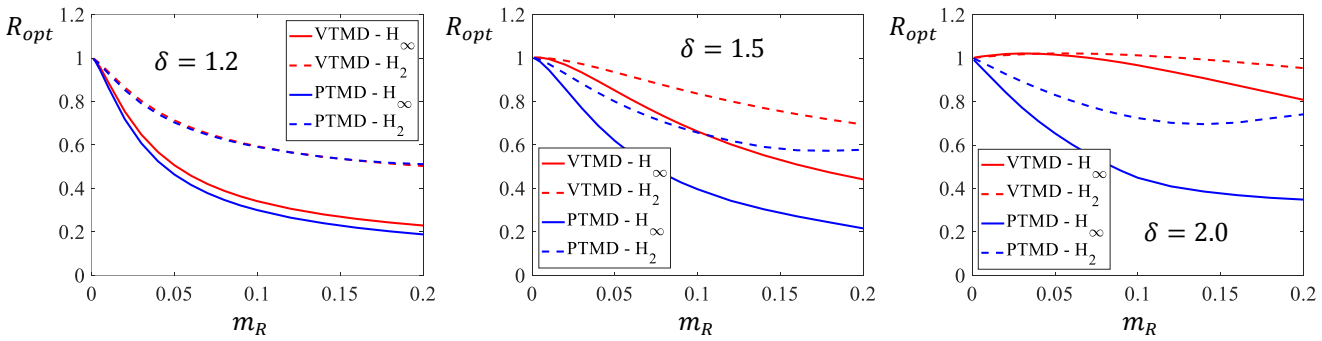

Figure 6: H_∞- and H_2-optimal VTMD and PTMD under ground acceleration: response ratios as a function of m_R, for increasing values of the frequency reduction factor δ.

Finally, referring to the 338 natural seismic records, Fig. 7 shows how frequency changes affect the mean spectral ratio of the structural displacement. The greater robustness of the PTMD is confirmed, the performance degradation being only slightly delayed. As δ increases, the PTMD becomes increasingly superior to the VTMD and the H_∞ design method becomes superior to the H_2 one.

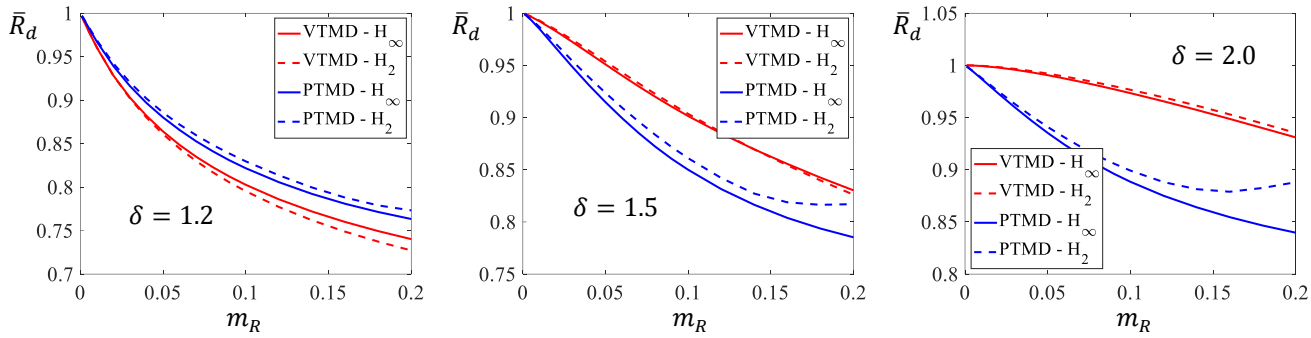

Figure 7: H_∞- and H_2-optimal VTMD and PTMD under the set of seismic records: mean spectral ratios in terms of max structural displacement as a function of m_R, for increasing values of the frequency reduction factor δ.

6. Conclusions

This paper examines the zero-gap PTMD as a possible variant to the traditional VTMD. After demonstrating the amplitude independence of the PTMD model, and setting and solving the H_∞ and H_2 optimum design problems, it compares the optimal PTMDs with the corresponding VTMDs, in different loading scenarios, with and without variations in the nominal structural frequency.

The results show that the PTMD is generally less effective than the VTMD if the structure responds as nominally expected, but sensibly more effective in the event of structural variations. They also show that the H_∞ design is less effective than the H_2 design in nominal conditions, but more robust against uncertainties. In conclusion, the zero-gap PTMD proves a promising alternative to traditional TMD types, and this study offers simple and effective solutions for its optimal seismic design.

REFERENCES

1 Matta, E. Seismic effectiveness and robustness of tuned mass dampers versus nonlinear energy sinks in a lifecycle cost perspective, *Bulletin of Earthquake Engineering*, **19** (1), 513–551, (2021).

2 Matta, E. Seismic effectiveness of tuned mass dampers in a life-cycle cost perspective, *Earthquake and Structures*, **9** (1), 73–91, (2015).

3 Nucera, F., Vakakis, A. F., McFarland, D. M., Bergman, L. A. and Kerschen, G. Targeted energy transfers in vibro-impact oscillators for seismic mitigation, *Nonlinear Dynamics*, **50**, 651–677, (2007).

4 Zhang, P., Song, G., Li, H.-N. and Lin, Y.-X. Seismic Control of Power Transmission Tower Using Pounding TMD, *Journal of Engineering Mechanics*, **139**(10), 1395–1406, (2013).

5 AL-Shudeifat, M. A., Wierschem N., Quinn D. D., Vakakis A. F., Bergman L. A. and Spencer Jr B. F. Numerical and experimental investigation of a highly effective single-sided vibro-impact non-linear energy sink for shock mitigation, *International Journal of Non-Linear Mechanics*, **52**, 96–109, (2013).

6 Wang, W., Hua, X., Wang, X., Chen, Z. and Song, G. Optimum design of a novel pounding tuned mass damper under harmonic excitation, *Smart Materials and Structures*, **26**, 055024, (2017).

7 Matta, E. A novel bidirectional pendulum tuned mass damper using variable homogeneous friction to achieve amplitude-independent control, *Earthquake Engineering and Structural Dynamics*, **48** (6), 653–677, (2019).